Shahid Beheshti University

Sustainable Earth Trends

Journal homepage: http://sustainearth.sbu.ac.ir

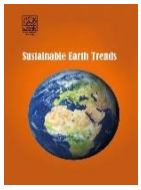

Refining airfoil designs: Tailored modifications for enhanced performance in low Reynolds number conditions

Hossein Seifi Davari[*a], Mohsen Seify Davari[b], Harun Chowdhury[c], Ruxandra Mihaela Botez[d]

[a] Department of Mechanical & Marine Engineering, Chabahar Maritime University, Chabahar, Iran b Faculty of Engineering and Technology, Islamic Azad University, Germi, Iran
[b] Faculty of Engineering and Technology, Islamic Azad University, Germi, Iran
[c] School of Engineering, RMIT University, Melbourne, VIC-3000, Australia
[d] Laboratory of Applied Research in Active Controls, Avionics, and AeroServoElasticity LARCASE, ÉTS-École de Technologie Supérieure, Université de Québec, Montréal, QC H3C 1K3, Canada

ABSTRACT

In the current study, three airfoils—PSU94-097, SD6060, and S2055—were analyzed for their aerodynamic performance across Reynolds numbers (Re) ranging from 50,000 to 500,000, typical for Small Wind Turbine (SWT) blade airfoils. Results indicated that as Re increased, the aerodynamic efficiency of all modified airfoils improved. Optimal thickness-to-camber ratios (t/c) of 1.50-2.25, 2.25-3, and 0.60-1.50 for SD6060, S2055, and PSU94-097 airfoils, respectively, contributed to enhanced efficiency. PSU94-097-modified airfoil demonstrated the highest lift-to-drag ratio (CL/CD) of 151.60 at Re of 500,000. Peak CL/CD values for SD6060-modified and S2055-modified airfoils were 109.87 and 97.13, respectively. PSU94-097-modified, SD6060-modified, and S2055-modified airfoils attained peak lift coefficients (CL) of 1.534, 1.219, and 1.174, respectively. PSU94-097-modified airfoil also showed the highest peak CL across Re ranging from 50,000 to 500,000. Percentage increase in peak CL/CD across Re range of 50,000 to 500,000 was 15.8%, 16.08%, 24.43%, 17.12%, 17.30%, 17.98%, and 20.22% for PSU94-097-modified airfoil; 27.87%, 2.03%, 13.77%, 15.83%, 15.14%, 17.95%, and 17.73% for SD6060-modified airfoil; and 16.70%, 7.11%, 5.77%, 7.25%, 11.40%, 9.99%, and 6.04% for S2055-modified airfoil. In addition to enhancing the aerodynamic efficiency of airfoils and consequently increasing electricity production in wind turbines, optimizing the t/c reduces the material needed for wind turbine construction. This not only lowers the cost but also minimizes environmental impact by using fewer resources. Thus, these modifications are environmentally beneficial, contributing to sustainable development alongside improving wind turbine efficiency.

ARTICLE INFO

Keywords:
Lift
Optimization
Reynolds Numbers
Turbine
Wind

Article history:
Received: 10 Jan 2024
Accepted: 12 Mar 2024

*corresponding author
E-mail address:
hseifidavary@cmu.ac.ir
(H. Seifi Davari)

Citation:
Seifi Davari, H. et al., (2024). Refining Airfoil Designs: Tailored Modifications for …, *Sustainable Earth Trends:* 4(2), (10-29).

DOI: 10.48308/set.2024.235573.1050

1. Introduction

SWTs are pivotal in converting renewable energy into electricity, offering versatile deployment options—standalone, grid-connected, or integrated into various systems (Seifi et al., 2023a). Due to their size and placement, SWTs excel in low Re airflows (Porto et al., 2022), typically operating below 500,000 Re (Seifi Davari et al., 2024a). Poorly designed blade airfoils can hamper aerodynamic performance, affecting wind turbine efficiency. Airfoils tailored for large turbines may not suit SWTs (Akour et al., 2018; Karthikeyan et al., 2015), necessitating optimization across parameters like CL, drag coefficient (CD), CL/CD, stall Angle of Attack (AoA), and drag bucket (Akour et al., 2018). Nemati and Jahangirian (2020) proposed a novel method for optimizing morphing wing segments, aiming to enhance high-lift capabilities while minimizing alterations. Utilizing a Genetic Algorithm (GA) and numerical solutions, they achieved superior

CL values in less computational time than traditional methods. Abdelwahed and El-Rahman (2020) applied shape optimization, using GA and XFOIL solver, to SG6043 airfoil, boosting CL/CD by up to 24% to 10% compared to the base design. Leite et al. (2022) aimed to develop a framework based on high-fidelity simulations to optimize the aerodynamic efficiency of a 2D simulation using a NACA0012 airfoil across various flight regimes, from subsonic to hypersonic speeds. Additionally, gradient-based optimizations were conducted to reduce drag. Their optimization results showcased a notable enhancement in aerodynamic efficiency compared to the baseline airfoil, with a reduction in CD of up to 79.2%. Bashir et al. (2022) selected the black widow optimization method for their investigation due to its superior performance among the explored optimization techniques. Their optimizations were performed to assess the impacts of different imposed constraints on optimization precision and to maximize CL/CD for cruising and climbing flight conditions, respectively. The CL/CD for the optimized airfoil relative to the standard airfoil in cruise flight conditions increased from 48.53 to 86.52, indicating that the optimized configurations outperformed the standard airfoil models. Tang et al. (2022) aimed to identify an ideal airfoil with minimal susceptibility to uncertainties while maintaining CL/CD compared to the standard airfoil. The optimized airfoil demonstrated a 17.96% decrease in the fluctuation spectrum without altering the mean CL/CD. Additionally, they employed a non-deterministic Computational Fluid Dynamics (CFD) method to validate the optimization process by analyzing the airflow domain. Additionally, Zargar et al. (2022) investigated two hybrid blade airfoils formed by merging the DU06W200 and NACA63215; their findings demonstrated that a novel hybrid blade airfoil could significantly alter the airflow pattern over the airfoil, resulting in increased aerodynamic efficiency. Research by Sarkar et al. (2023) suggests that airfoils with slots demonstrate higher lift and power coefficients (Cp) compared to those without slots. They evaluated the effectiveness of SWT blades by analyzing the NACA0018 airfoil and a slotted airfoil configuration. Efficiency notably improved when slots were integrated into the basic airfoil at an AoA of 15°, resulting in increases of 2.32% and 17.94% in CL and Cp, respectively. Lendraitis and Lukoševičius (2023) optimized the CL/CD ratio of the NACA23012 airfoil flap using the suggested airfoil parameters method. Starting at 0.7c with a 10° deflection, their study employed a GA to shape a morphing trailing-edge flap, enabling aerodynamic optimization while capturing the expected structural behavior. The optimizer produced a structurally feasible morphing flap that enhanced the CL/CD within the optimized AoA range by 10%. Bhavsar et al. (2023) investigated the impact of slots on the CL and CD of an airfoil across various AoAs by examining an innovative slot design for the DU-99-W405 airfoil shape. Five different slot positions along the chord were analyzed, revealing that the slot 2 configuration yielded the highest CL, CD, and CL/CD values, with significant improvements. Salinas et al. (2023) demonstrated the potential enhancement in CL/CD achievable through the GA method, while Longtin Martel et al. (2023) observed a significant increase in overall aerodynamic efficiency in developed airfoils. Sefi Davari et al. (2023) examined the aerodynamic performance of various airfoils by modifying their shapes using XFOIL software across a range of Re. They found that the NACA0015 airfoil exhibited a high peak CL/CD at low Re, with XFOIL predictions closely matching wind tunnel experiments. Tanürün (2024) showed that adaptive flap design enhanced efficiency by enlarging the wake and intensifying vortices behind the turbine blade. Despite numerous significant studies on airfoil optimization that enhance aerodynamic performance using various tools, research specifically focusing on t/c and its impact on aerodynamic effectiveness remains limited. This study investigates the modification of PSU94-097, SD6060, and S2055 airfoils, analyzing their aerodynamic performance characteristics under low Re conditions and varying wind velocities. The aerodynamic capabilities of the modified PSU94-097, SD6060, and S2055 airfoils, along with their improved effectiveness across a range of Re conditions from 50,000 to 500,000, are examined in this study. This Re range corresponds to the typical performance region of SWTs (Kumar and Narayanan, 2022). Following an introduction to airfoil optimization, CL, CD, drag bucket, and maximum CL/CD for both the original and modified airfoils are discussed, highlighting the optimal t/c for each airfoil across the Re range

of 50,000 to 500,000. Additionally, the validity of the study is confirmed by comparing its findings with those of other researchers. These findings lay the groundwork for developing additional low Re airfoils and underscore the essential aerodynamic characteristics of the modified PSU94-097, SD6060, and S2055 airfoils. The methods employed in conducting this research are detailed in the subsequent section.

2. Material and Methods

2.1. Selection of the Airfoil

In a recent study, wind turbine (WT) blades were targeted for enhancement using a gradient-based shape optimization method. This method integrates Blade Element Momentum (BEM) theory with a 2D potential airflow solver that incorporates viscous effects and XFOIL. The power output of the WT, analyzed through the BEM analyzer, serves as the objective parameter for the gradient-based optimization method. XFOIL, a commonly used tool by researchers for airfoil design and analysis, has been supported by previous studies (Song and David Lubitz, 2014; Seifi et al., 2023b; Bai et al., 2014; Seifi Davari et al., 2024b; Seifi Davari et al., 2023b) for its efficiency impacts. Considering their superior aerodynamic effectiveness in low Re conditions, the SD6060 (Tarhan and Yilmaz, 2019), PSU94-097 (Maughmer et al., 2002), and S2055 (Badawy et al., 2023) airfoils were chosen as the foundation for generating new airfoils in this study. Using XFOIL, the thickness and camber parameters of the original airfoils were adjusted to reshape their key features and create innovative designs. For each t/c setting, the newly developed airfoil with the maximum CL/CD at Re between 50,000 and 500,000 was examined. The geometric characteristics of the newly created airfoils were then determined based on the t/c area with the highest CL/CD. Each t/c configuration, along with the best-performing new airfoil, underwent testing to determine the peak CL/CD at Re ranging from 50,000 to 500,000. Further definition of the geometric characteristics of the specific modified airfoils was achieved using a t/c region with a higher CL/CD. Parameters for the aerodynamic effectiveness of the novel modified airfoils were identified and compared to the baseline airfoil at Re between 50,000 and 500,000. These parameters included CL, CD, CL/CD, stall AoA, and drag buckets. Fig. 1 outlines the experimental method used for the innovative airfoil designs in XFOIL. Studies of airfoil performance were conducted for viscous airflow with Re ranging from 50,000 to 500,000 and AoA ranging from 0° to 20°. Section 3 presents examples of the new performance standards for innovative airfoils.

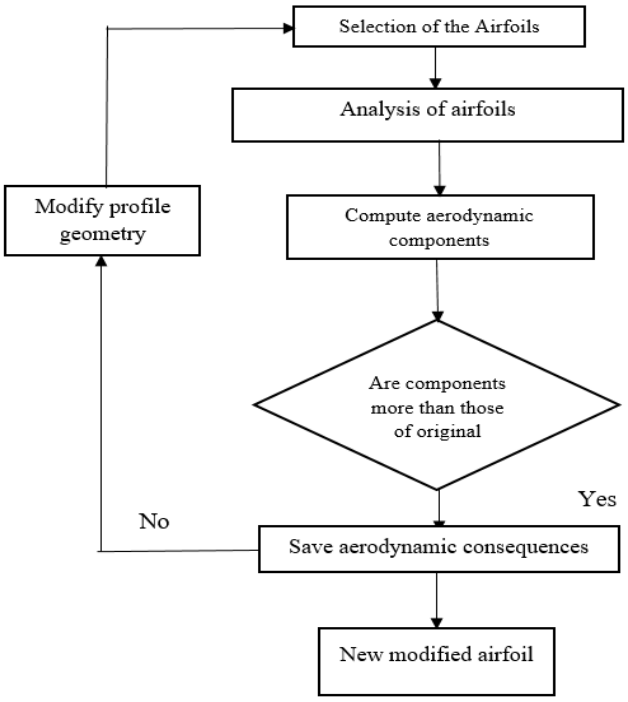

Fig. 1. Abstract of XFOIL process for profile experiment

2.2. Airfoils Modified Optimization

2.2.1. SD6060 Airfoil Modified Optimization

In the current study, the CL/CD efficiency of various airfoil t/c values served as the basis for optimizing modified airfoils. Initial optimization results for the SD6060 airfoil revealed differences in the peak CL/CD across different t/c values at Re ranging from 50,000 to 500,000, as shown in Fig. 2. At each Re, the peak CL/CD exhibited a dome-shaped relationship with t/c, with CL/CD efficiency generally increasing as Re increased. The highest point of peak CL/CD occurred within the t/c range of 1.50 to 2.25 for each Re. Consequently, outside this t/c range, peak CL/CD tended to decrease. The t/c range analyzed during the development of the airfoils in this study was 1.50 to 2.25, which was used to determine the thicknesses and camber of the SD6060 airfoil. As depicted in Fig. 2(b), the optimization of the SD6060 airfoil results in a peak thickness of 7.34% at 24.80% of the chord and a peak camber of 3.67% at 43.20% of the chord. Conversely, the peak thickness and camber of the modified SD6060 airfoils are 10.37% at 33.92% of the chord and 1.85% at 38.52% of the chord, respectively. This graph highlights the primary differentiating factor between the SD6060 airfoil and its modified counterparts: the geometrical features of thickness and camber. Specifically, the modified SD6060 airfoils exhibit thinner and more cambered designs compared to the original SD6060 airfoil.

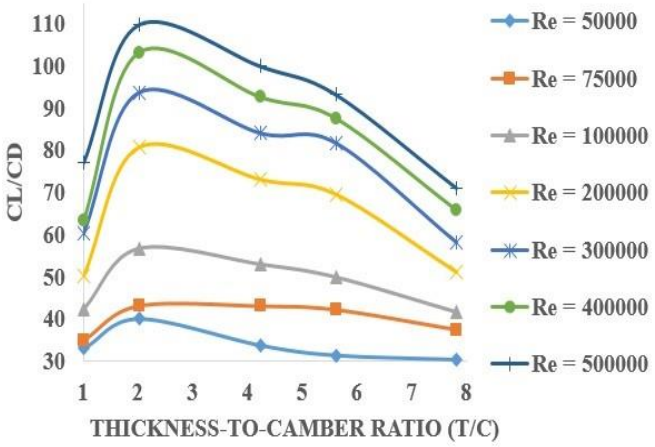

a) Peak CL/CD at various t/c

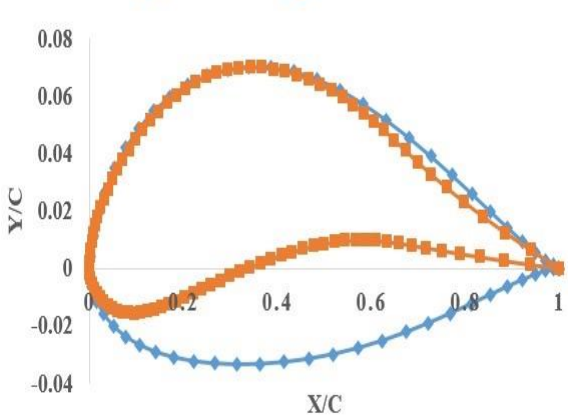

b) SD6060 and SD6060modified airfoils

Fig. 2. Airfoil geometry variation for SD6060 airfoil optimization

2.2.2. S2055 Airfoil Modified Optimization

Based on preliminary design optimization results, Fig. 3(a) illustrates the variations in peak CL/CD with t/c for the S2055 airfoil across Re ranging from 50,000 to 500,000. It can be observed from Fig. 3(a) that the peak CL/CD exhibited a dome-shaped relationship with t/c for each Re, indicating that the efficiency of CL/CD generally improved with increasing Re. The peak CL/CD occurred at its maximum for each Re within the t/c range of 2.25 to 3. Consequently, the peak CL/CD was observed to

decrease outside of this t/c range. The thickness and camber of the S2055 airfoil were determined based on the t/c, which was considered during the development of the airfoils in the current research. Specifically, the t/c ranged from 2.25 to 3.

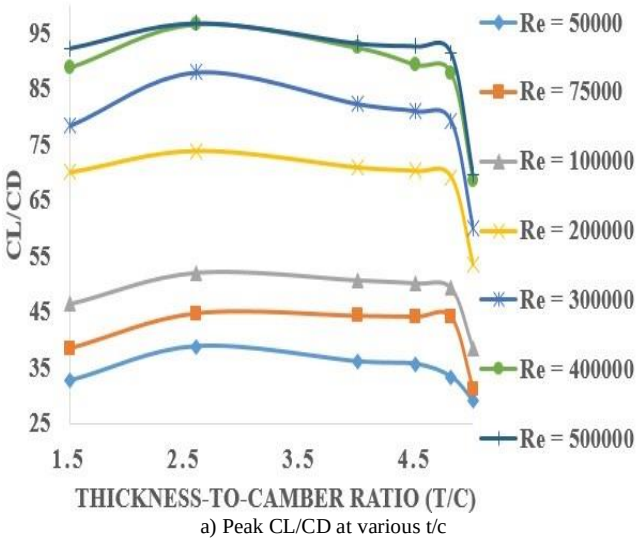

a) Peak CL/CD at various t/c

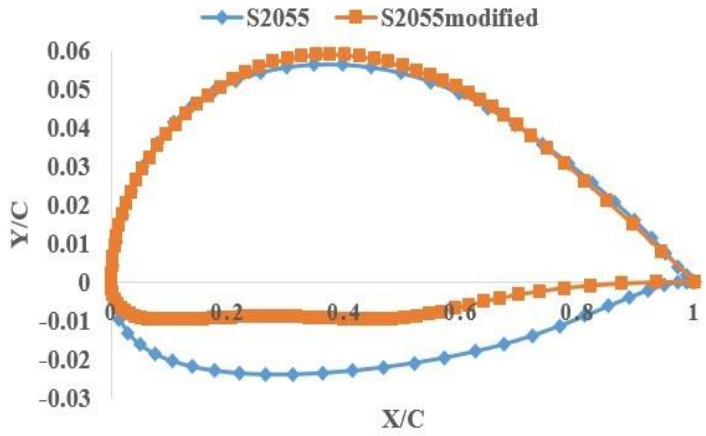

b) S2055 and S2055modified airfoils

Fig. 3. Airfoil geometry variation for S2055 airfoil optimization

As depicted in Fig. 3(b), the optimization of the S2055 airfoil results in a peak thickness of 6.84% at 37.70% of the chord and a peak camber of 2.49% at 35.10% of the chord. Additionally, the camber of the S2055 airfoil peaks at 1.66% at 44.61% of the chord, while the thickness peaks at 7.99% at 34.81% of the chord. The primary distinction between the S2055 airfoil and its modified counterparts lies in the geometrical features of thickness and camber, as illustrated in Fig. 3(b). Specifically, the modified S2055 airfoils exhibit thinner and more cambered designs compared to the original S2055 airfoil.

2.2.3. PSU94-097 Airfoil Modified Optimization

Based on early design optimization results, Fig. 4(a) illustrates the variations in peak CL/CD with t/c for the PSU94-097 airfoil across Re ranging from 50,000 to 500,000. Fig. 4(a) reveals that the peak CL/CD exhibited a dome-shaped relationship with t/c for each Re, indicating an overall improvement in CL/CD efficiency with increasing Re. The peak CL/CD occurred at its maximum for each Re within the t/c range of 0.60 to 1.50. Consequently, the peak CL/CD was observed to decrease outside of this t/c range. The thickness and camber of the PSU94-097 airfoil were determined based on the t/c, which was taken into account during the development of the airfoils in the current research. Specifically, the t/c ranged from 0.60 to 1.50. Therefore, the peak CL/CD was reduced outside this t/c range. The t/c range of 0.60-1.50, considered during the development of the airfoils in this study, was used to determine the thickness and camber of the PSU94-097 airfoil.

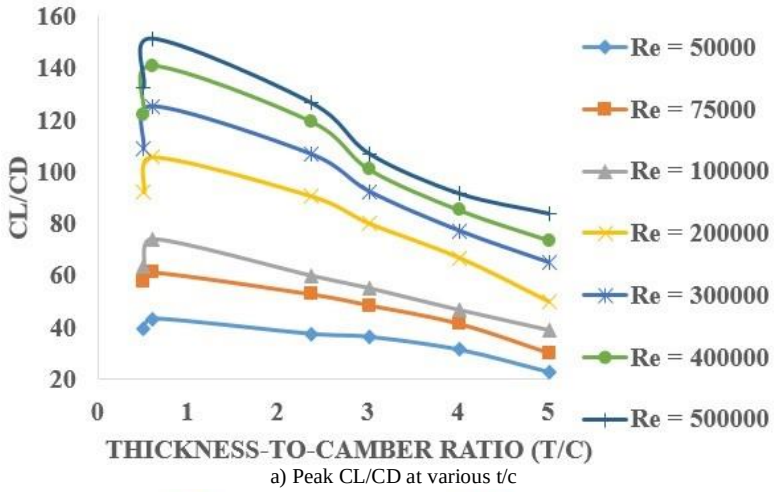

a) Peak CL/CD at various t/c

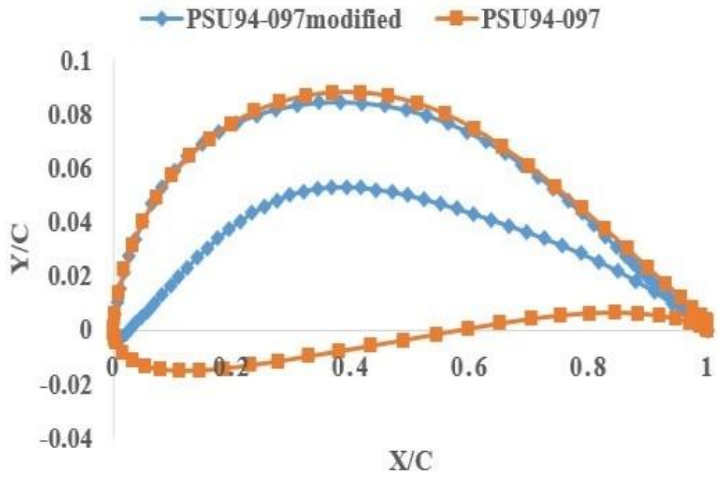

b) PSU94-097 and PSU94-097modified airfoils

Fig. 4. Airfoil geometry variation for PSU94-097 airfoil optimization

Graphically depicted in Fig. 4(b), the optimization of the PSU94-097 airfoil results in a peak thickness of 4.13% at 12.40% of the chord and a peak camber of 6.88% at 38.20% of the chord. Additionally, the camber peaks at 4.10% at 46.30% of the chord, while the thickness peaks at 9.70% at 32.30% of the chord for the PSU94-097 airfoil. The primary distinction between the PSU94-097 airfoil and its modified counterpart lies in the geometrical features of thickness and camber, as illustrated in Fig. 4(b). Specifically, the modified PSU94-097 airfoil features designs that are more cambered and thinner compared to the original PSU94-097 airfoil.

3. Results and discussion

3.1. Validation data

As illustrated in Figs. 5(a) and 5(b), the aerodynamic efficiency of the E387 airfoil, as predicted by X-Foil at Re of 200,000 and 400,000, is compared with experimental and XFOIL data from Wei et al. (2020) to confirm the accuracy of XFOIL. The results from both the experiment and XFOIL demonstrate strong agreement, supporting the reliability of XFOIL for further optimization purposes.

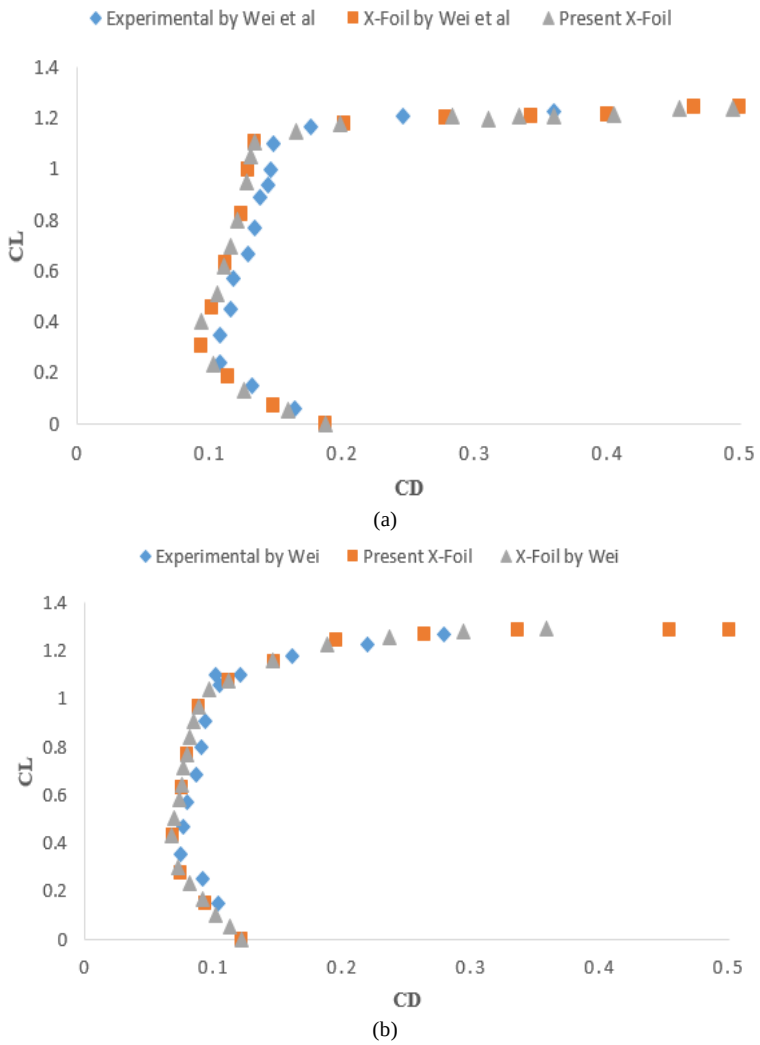

Fig. 5. Variation of aerodynamic parameters predicted by the X-FOIL data and experimental findings (Wei et al., 2020)

3.2. Comparison of CL, drag buckets, and CL/CD of basic airfoils with modified airfoils

In Fig. 6(a), the CL efficiency graph of the base and modified airfoils at a Re of 50,000 is depicted. It is evident from Fig. 6(a) that the CL of the PSU94-097 modified airfoils is higher than that of the other airfoils. Specifically, the PSU94-097 modified airfoil outperforms the original and other modified airfoils in CL investigations, particularly for AoAs ranging from 0° to 20°. Furthermore, the PSU94-097 modified airfoil achieved a peak CL of 1.534 at an AoA of 9°. In comparison, the SD6060 modified and S2055 modified airfoils reached maximum CL values of 1.155 at an AoA of 9° and 0.98 at an AoA of 8°, respectively. On the other hand, the peak CL values for the PSU94-097 airfoil at an AoA of 12°, the SD6060 airfoil at an AoA of 10°, and the S2055 airfoil at an AoA of 8° were 1.371, 1.016, and 0.929, respectively. Fig. 6(b) demonstrates that the PSU94-097 modified airfoil exhibited better drag characteristics compared to the entire airfoil at a Re of 50,000. While all original and modified airfoils experienced gradual increases in lift without corresponding increases in drag initially, the drag for the PSU94-097 and PSU94-097 modified airfoils began to increase dramatically above a CL of 0.47. Similarly, for the SD6060 modified, SD6060, S2055, and S2055 modified airfoils, initial lift increments occurred gradually without accompanying increases in drag, but drag began to rise abruptly above a CL of 0.035. Notably, differences in performance among the PSU94-097 modified airfoils became more pronounced above a CD of 0.0356, with the PSU94-097 modified airfoil exhibiting the best performance in the drag bucket, followed by the SD6060 modified and S2055 modified airfoils.

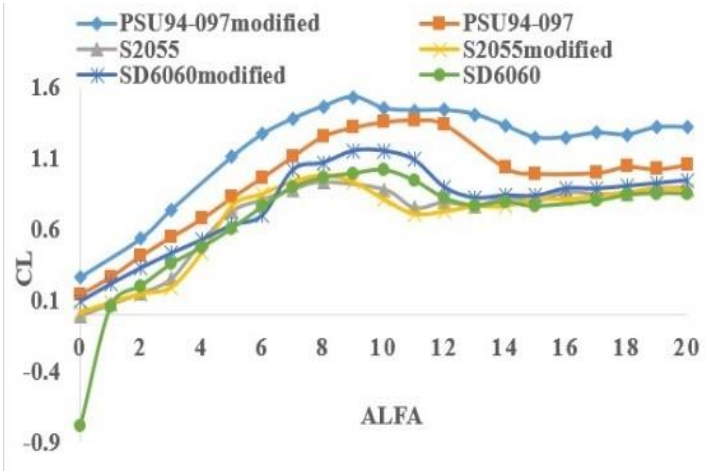

a) CL of base and modified airfoils

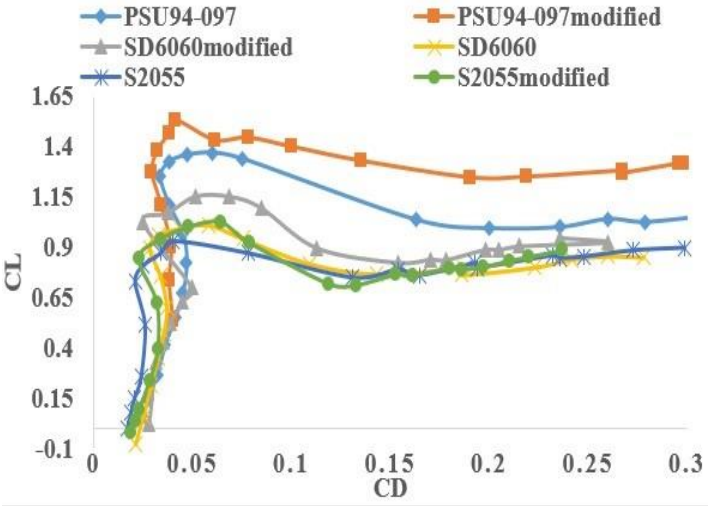

b) Drag buckets for base and modified airfoils

Fig. 6. Comparison of CL, drag buckets, and CL/CD of base and modified airfoils at Re of 50,000

Fig. 6(c) illustrates the CL/CD performance of the original and modified airfoils at a Re of 50,000. According to Fig. 6(c), the PSU94-097 modified airfoil outperforms the original and other modified airfoils in CL/CD investigations, particularly for AoAs ranging from 2° to 7°. The highest maximum CL/CD of 43.20 was recorded by the PSU94-097 modified airfoil at an AoA of 6°, while the lowest value was obtained by the SD6060 airfoil at an AoA of 7°, where it measured 31.43. Additionally, the greatest CL/CD values for the SD6060 modified and S2055 modified airfoils were 40.19 at an AoA of 7° and 38.85 at an AoA of 5°, respectively. Moreover, the highest CL/CD values for the PSU94-097 and S2055 airfoils were 37.33 at an AoA of 8° and 33.29 at an AoA of 5°. Hence, the maximum CL/CD of all modified airfoils exceeded that of their original counterparts. Fig. 7(a) displays the CL efficiency graph of the base and modified airfoils at a Re of 75,000. The PSU94-097 modified airfoil again exhibits higher CL values compared to the other airfoils, particularly for AoA ranging from 1° to 20°. Moreover, the PSU94-097 modified airfoil achieved a peak CL of 1.498 at an AoA of 12°. Additionally, the SD6060 modified and S2055 modified airfoils reached peak CL values of 1.168 at an AoA of 10° and 1.038 at an AoA of 9°, respectively. Meanwhile, the peak CL values for the PSU94-097 airfoil at an AoA of 11°, the SD6060 airfoil at an AoA of 10°, and the S2055 airfoil at an AoA of 9° were 1.374, 1.02, and 0.963, respectively. Furthermore, the PSU94-097 modified airfoil exhibited the highest stall AoA of 12°. In Fig. 7(b), it is demonstrated that the PSU94-097 modified airfoil exhibited better drag characteristics compared to the entire set of airfoils at a Re of 75,000. Initially, all original and modified airfoils experienced gradual increases in lift without corresponding increases in drag, although the drag for the PSU94-097 and PSU94-097 modified airfoils began to increase dramatically above a CL of 1.20. Similarly, for the SD6060 modified, SD6060,

S2055, and S2055 modified airfoils, initial lift increments occurred gradually without accompanying increases in drag, but drag began to rise abruptly above a CL of 0.434. Notably, performance differences among the PSU94-097 modified airfoils became more pronounced above a CD of 0.0205, with the PSU94-097 modified airfoil exhibiting the best performance in the drag bucket, followed by the SD6060 modified and S2055 modified airfoils.

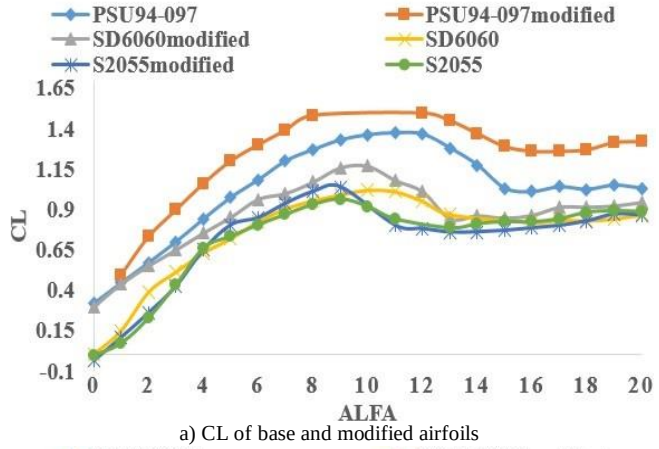

a) CL of base and modified airfoils

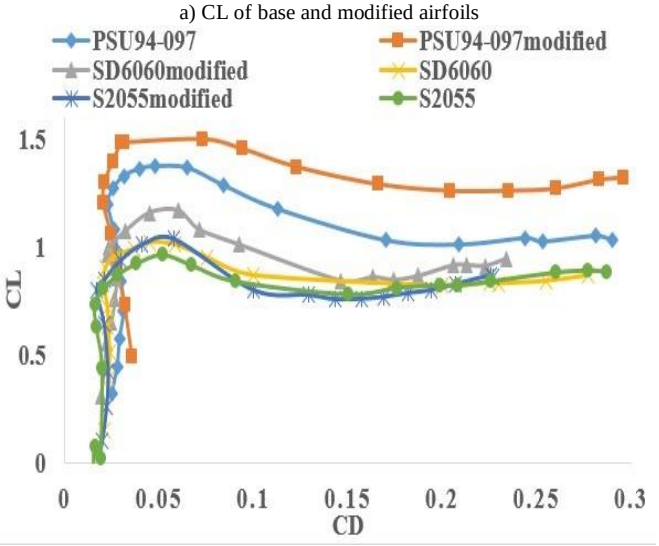

b) Drag buckets for base and modified airfoils

Fig. 7. Comparison of CL, drag buckets, and CL/CD of base and modified airfoils at Re of 75,000

Fig. 7(c) illustrates the CL/CD efficiency of the base and modified airfoils at a Re of 75,000. According to Fig. 7(c), the PSU94-097 modified airfoil outperforms the base and other modified airfoils in CL/CD investigations, particularly for AoAs between 2° and 7°. The highest peak CL/CD of 61.14 was achieved by the PSU94-097 modified airfoil at an AoA of 6°, while the lowest value was recorded by the SD6060 airfoil at an AoA of 7°, measuring 42.34. Additionally, the greatest CL/CD values for the S2055 modified and SD6060 modified airfoils were 47.10 at an AoA of 5° and 43.20 at an AoA of 7°, respectively. Similarly, the peak CL/CD values for the PSU94-097 and S2055 airfoils were 52.67 at an AoA of 7° and 43.97 at an AoA of 5°. Therefore, the maximum CL/CD of all modified airfoils exceeded that of their base counterparts. Fig. 8(a) depicts the CL efficiency graphs of the base and modified airfoils at Re of 100,000. The PSU94-097 modified airfoil exhibits higher CL values compared to the other airfoils. It outperforms the base and other modified airfoils in CL investigations, especially for AoA ranging from 1° to 20°. Additionally, the peak CL of the PSU94-097 modified airfoil was 1.50 at an AoA of 12°. Moreover, the SD6060 modified and S2055 modified airfoils achieved peak CL values of 1.174 at an AoA of 10° and 1.057 at an AoA of 9°, respectively, while the peak CL of the PSU94-097 airfoil at an AoA of 12°, the SD6060 airfoil at an AoA of 11°, and the S2055 airfoil at an AoA of 8° were 1.379, 1.03, and 0.938, respectively. Additionally, the PSU94-097 modified airfoil exhibited the greatest stall

AoA of 12°. In Fig. 8(b), it is demonstrated that the PSU94-097 modified airfoil exhibited better drag characteristics compared to all other airfoils at Re of 100,000. Initially, all base and modified airfoils experienced gradual increases in lift without corresponding increases in drag, although the drag for the PSU94-097 and PSU94-097 modified airfoils began to increase dramatically above a CL of 1.10. Similarly, for the SD6060 modified, SD6060, S2055, and S2055 modified airfoils, initial lift increments occurred gradually without accompanying increases in drag, but drag began to rise abruptly above a CL of 0.731. Notably, performance differences among the PSU94-097 modified airfoils became more pronounced above a CD of 0.018, with the PSU94-097 modified airfoil performing best in the drag bucket, followed by the SD6060 modified and S2055 modified airfoils.

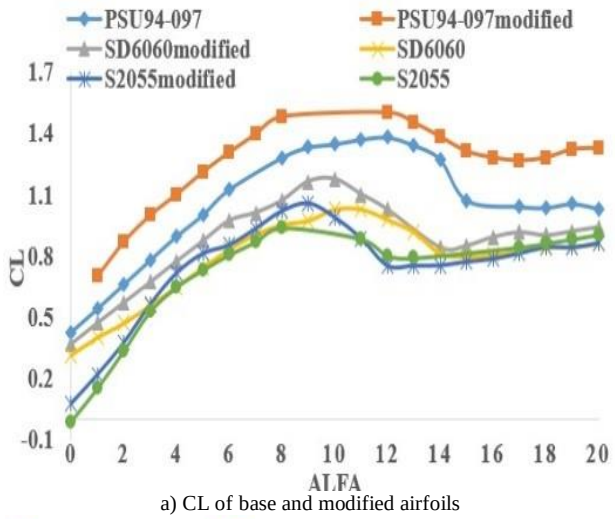

a) CL of base and modified airfoils

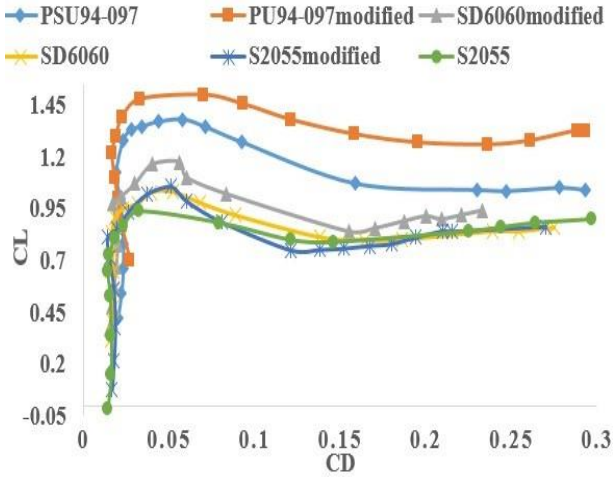

b) Drag buckets for base and modified airfoils

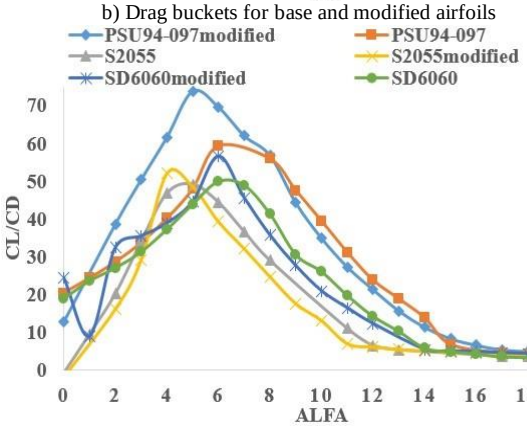

c) CL/CD performance of base and modified airfoils

Fig. 8. Comparison of CL, drag buckets, and CL/CD of base and modified airfoils at Re of 100,000

Fig. 8(c) illustrates the CL/CD efficiency of the base and modified airfoils at a Re of 100,000. For AoAs ranging from 1° to 8°, the PSU94-097 modified airfoil outperforms the base and other modified airfoils in CL/CD investigations. At an AoA of 5°, the PSU94-097 modified airfoil displayed the highest peak CL/CD of 73.84, while the S2055 airfoil recorded the lowest value of 49.20 at the same AoA. Furthermore, the highest CL/CD values for the modified SD6060 and S2055 airfoils were 56.66 at an AoA of 6° and 52.04 at an AoA of 4°, respectively. Additionally, for the PSU94-097 and SD6060 airfoils, the maximum CL/CD values were 73.84 at an AoA of 5° and 49.80 at an AoA of 6°, respectively. Consequently, all modified airfoils exhibited a higher maximum CL/CD than their base airfoils. Fig. 9(a) presents the CL efficiency graphs of the base and modified airfoils at Re of 200,000. The PSU94-097 modified airfoil demonstrates higher CL values compared to other airfoils. It outperforms the base and other modified airfoils in CL investigations, particularly for AoA ranging from 0° to 11°. Additionally, the peak CL of the PSU94-097 modified airfoil was 1.49 at an AoA of 10°. Moreover, the SD6060 modified and S2055 modified airfoils achieved peak CL values of 1.19 at an AoA of 10° and 1.07 at an AoA of 9°, respectively, while the peak CL of the PSU94-097 airfoil at an AoA of 12°, the SD6060 airfoil at an AoA of 11°, and the S2055 airfoil at an AoA of 10° were 1.394, 1.045, and 1.016, respectively. In Fig. 9(b), it is demonstrated that the PSU94-097 modified airfoil exhibits better drag characteristics compared to all other airfoils at Re of 200,000. Initially, all base and modified airfoils experience gradual increases in lift without corresponding increases in drag, although the drag for the PSU94-097 and PSU94-097 modified airfoils begins to increase dramatically above a CL of 1.136. Similarly, for the SD6060 modified, SD6060, S2055, and S2055 modified airfoils, initial lift increments occur slowly without accompanying increases in drag, but drag begins to rise abruptly above a CL of 0.576. Notably, performance differences among the PSU94-097 modified airfoils become more pronounced above a CD of 0.015, with the PSU94-097 modified airfoil performing best in the drag bucket, followed by the SD6060 modified and S2055 modified airfoils.

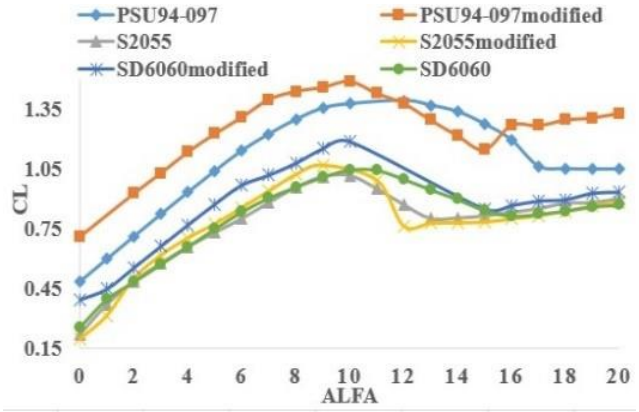

a) CL of base and modified airfoils

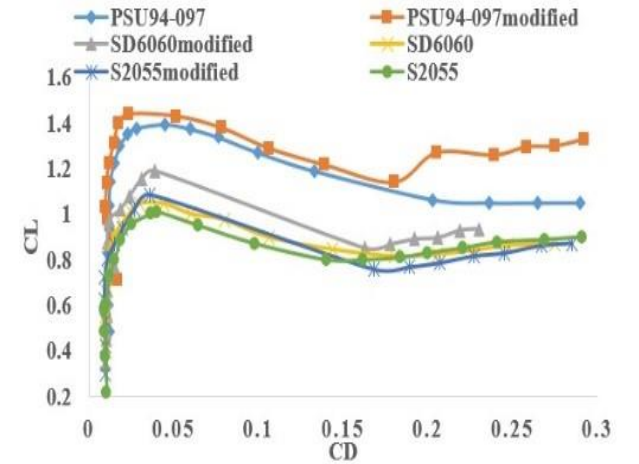

b) Drag buckets for base and modified airfoils

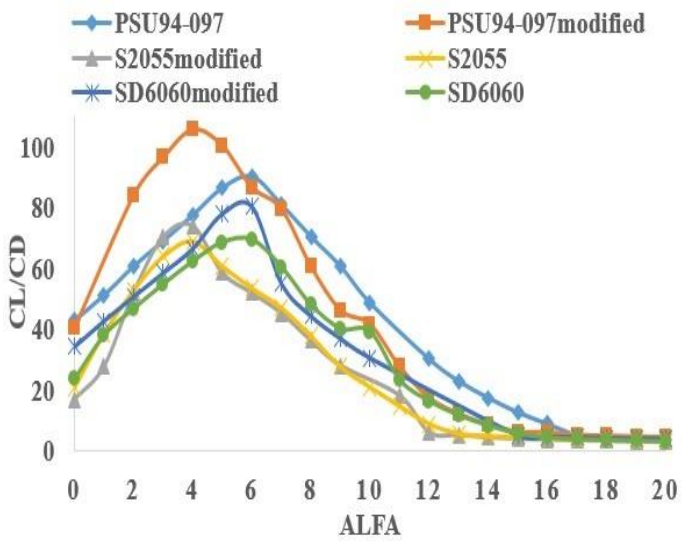

c) CL/CD performance of base and modified airfoils

Fig. 9. Comparison of CL, drag buckets, and CL/CD of base and modified airfoils at Re of 200,000

Fig. 9(c) illustrates the CL/CD efficiency of the base and modified airfoils at Re of 200,000. The PSU94-097 modified airfoil outperforms the base and other modified airfoils in CL/CD investigations for AoA ranging from 0° to 5°. At an AoA of 4°, the PSU94-097 modified airfoil exhibited the highest peak CL/CD of 105.96, while the S2055 airfoil showed the lowest value of 69.17. Similarly, the highest CL/CD values for the SD6060 modified and S2055 modified airfoils were 80.54 at an AoA of 6° and 74.19 at an AoA of 4°, respectively. Additionally, at an AoA of 6°, the greatest CL/CD values for the PSU94-097 and SD6060 airfoils were 90.47 and 69.53, respectively. Consequently, all modified airfoils exhibited a greater maximum CL/CD compared to the base airfoils. The CL efficiency graphs of the base and modified airfoils at Re of 300,000 are presented in Fig. 10(a). The PSU94-097 modified airfoil demonstrates higher CL values compared to other airfoils. It outperforms the base and other modified airfoils in CL investigations, particularly for AoA ranging from 0° to 20°. Additionally, the peak CL of the PSU94-097 modified airfoil was 1.497 at an AoA of 10°. Moreover, the SD6060 modified and S2055 modified airfoils achieved peak CL values of 1.172 at an AoA of 10° and 1.125 at an AoA of 10°, respectively, while the peak CL of the PSU94-097 airfoil at an AoA of 12°, the SD6060 airfoil at an AoA of 11°, and the S2055 airfoil at an AoA of 9° were 1.434, 1.08, and 1.03, respectively. Consequently, the stall AoA of the S2055 modified airfoil has increased from 9° to 10°. In Fig. 10(b), it is evident that the PSU94-097 modified airfoil exhibits better drag characteristics compared to all other airfoils at Re of 300,000. Initially, all base and modified airfoils experience gradual increases in lift without corresponding increases in drag, although the drag for the PSU94-097 and PSU94-097 modified airfoils begins to increase dramatically above a CL of 1.138. Similarly, for the SD6060 modified, SD6060, S2055, and S2055 modified airfoils, initial lift increments occur slowly without accompanying increases in drag, but drag begins to rise abruptly above a CL of 0.649. Notably, performance differences among the PSU94-097 modified airfoils become more pronounced above a CD of 0.0130, with the PSU94-097 modified airfoil performing best in the drag bucket, followed by the SD6060 modified and S2055 modified airfoils.

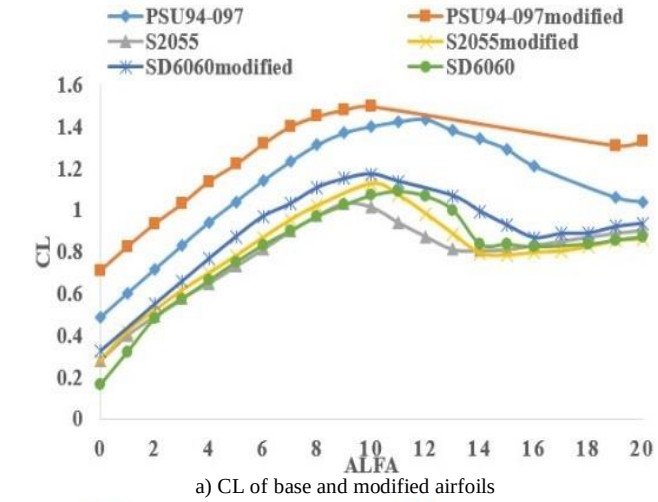

a) CL of base and modified airfoils

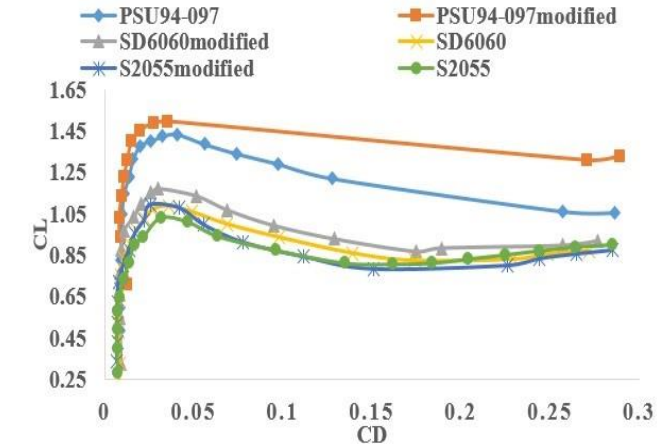

b) Drag buckets for base and modified airfoils

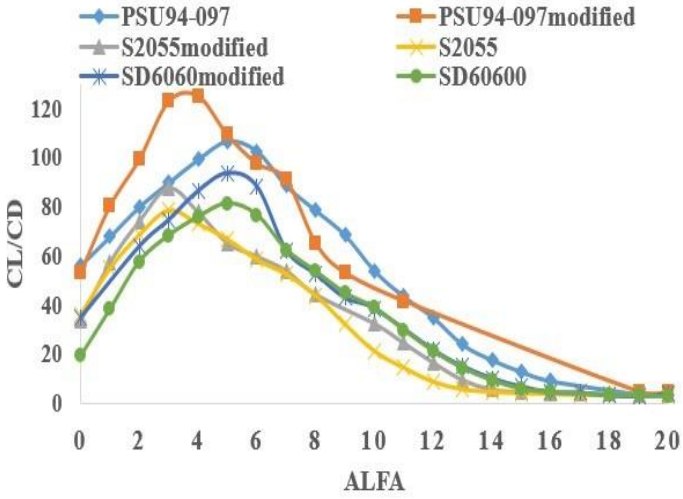

c) CL/CD performance of base and modified airfoils

Fig. 10. Comparison of CL, drag buckets, and CL/CD of base and modified airfoils at Re of 300,000

The CL/CD efficiency of the base and modified airfoils at Re of 300,000 is depicted in Fig. 10(c). In analyses for AoA from 1° to 5°, the PSU94-097 modified airfoil outperforms the base and other modified airfoils. It achieved the highest peak CL/CD of 125.40 at an AoA of 4°, while the S2055 airfoil exhibited the lowest value of 78.92. Similarly, the highest CL/CD values for the SD6060 modified and S2055 modified airfoils were 93.84 at an AoA of 5° and 87.92 at an AoA of 3°, respectively. Additionally, the highest CL/CD values for the PSU94-097 and SD6060 airfoils were 106.90 and 81.50, respectively, at an AoA of 6°. Therefore, all modified airfoils had a higher maximum CL/CD than the base airfoils.

Fig. 11(a) illustrates the CL performance graphs of the base and modified airfoils at a Re of

400,000. The modified PSU94-097 airfoil exhibited greater CL values than the conventional airfoils. It outperforms the base and other modified airfoils in CL investigations, particularly for AoA ranging from 0° to 20°. Likewise, with an AoA of 10°, the highest CL of the PSU94-097 modified airfoil was 1.508. The maximum CL of the PSU94-097 airfoil at an AoA of 11°, the SD6060 airfoil at an AoA of 11°, and the S2055 airfoil at an AoA of 9° were 1.45, 1.115, and 1.047, respectively, while for the SD6060 and S2055 modified airfoils, they were 1.194 and 1.151 at an AoA of 10°, respectively. Consequently, the stall AoA of the S2055 modified airfoil has increased from 9° to 10°. Fig. 11(b) indicates that the PSU94-097 modified airfoil exhibited better drag characteristics than all other airfoils at a Re of 400,000. Initially, all original and modified airfoils experienced gradual increases in lift without corresponding increases in drag; however, the drag for the PSU94-097 and PSU94-097 modified airfoils began to increase dramatically above a CL of 1.10. Similarly, for the SD6060 modified, SD6060, S2055, and S2055 modified airfoils, initial lift increments occurred slowly without accompanying increases in drag, but drag began to rise abruptly above a CL of 0.729. Notably, the efficiency differences among the PSU94-097 modified airfoils mostly appear above the CD of 0.0124, where the PSU94-097 modified airfoil performs best in the drag bucket, followed by the SD6060 modified and S2055 modified airfoils.

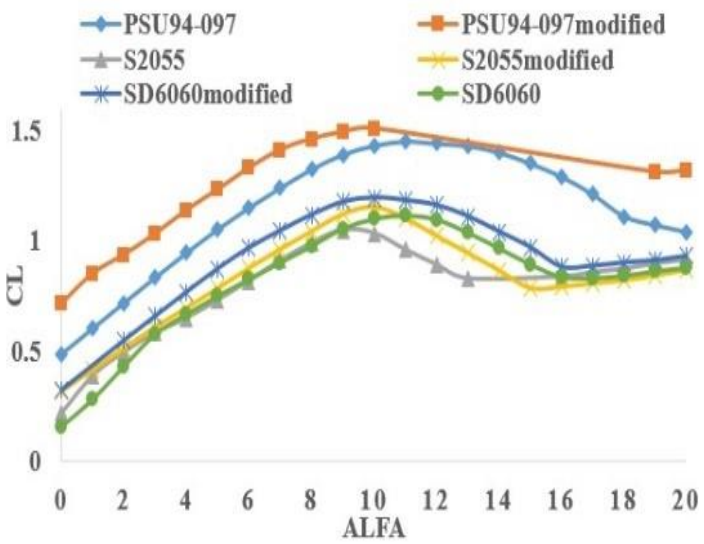

a) CL of base and modified airfoils

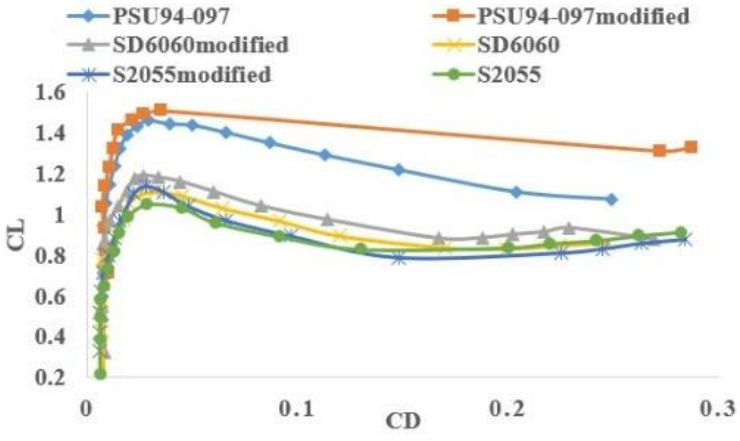

b) Drag buckets for base and modified airfoils

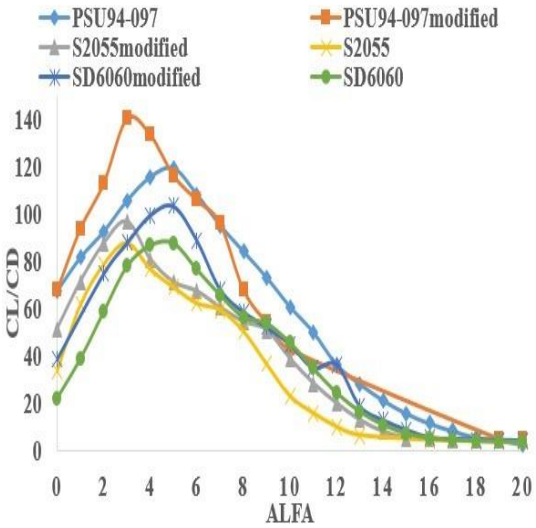

c) CL/CD performance of base and modified airfoils

Fig. 11. Comparison of CL, drag buckets, and CL/CD of base and modified airfoils at Re of 400,000

Fig. 11(c) illustrates the CL/CD efficiency of the original and modified airfoils at a Re of 400,000. The PSU94-097 modified airfoil outperforms the base and other modified airfoils in studies for AoA from 1° to 4°. It achieved a maximum CL/CD of 140.40 at an AoA of 4°, while the SD6060 airfoil reached a maximum CL/CD of 87.52 at an AoA of 5°. Similarly, the highest CL/CD values for the S2055 modified and SD6060 modified airfoils were 103.23 at an AoA of 5° and 96.60 at an AoA of 3°, respectively. For the PSU94-097 and SD6060 airfoils, the greatest CL/CD values were 119 at an AoA of 5° and 87.81 at an AoA of 3°, respectively. Consequently, all modified airfoils exhibited a higher maximum CL/CD than the basic airfoils. Fig. 12(a) illustrates the CL performance graphs of the base and modified airfoils at a Re of 500,000. The PSU94-097 modified airfoil demonstrated a higher CL than the conventional airfoils. It performed better in CL investigations, particularly for AoA ranging from 0° to 10°, in comparison to the base and other modified airfoils. Similarly, at an AoA of 10°, the highest CL of the PSU94-097 modified airfoil was 1.52. The maximum CL of the PSU94-097 airfoil at an AoA of 11°, the SD6060 airfoil at an AoA of 11°, and the S2055 airfoil at an AoA of 9° were each 1.489, 1.138, and 1.058, respectively, while for the SD6060 and S2055 modified airfoils, they were 1.219 at an AoA of 10° and 1.174 at an AoA of 10°, respectively. Consequently, the stall AoA of the S2055 modified airfoil has increased from 9° to 10°. Fig. 12(b) shows that the PSU94-097 modified airfoil exhibited better drag characteristics than the entire airfoil at a Re of 500,000. Initially, all base and modified airfoils experienced gradual increases in lift without corresponding increases in drag; however, the drag for the PSU94-097 and PSU94-097 modified airfoils began to rise dramatically above a CL of 1.10. Similarly, for the SD6060 modified, SD6060, S2055, and S2055 modified airfoils, initial lift increments occurred slowly without accompanying increases in drag, but the drag on the airfoils began to rise abruptly above a CL of 0.71. Notably, the efficiency differences among the PSU94-097 modified airfoils mostly became apparent above the CD of 0.0344, where the PSU94-097 modified airfoil performed best in the drag bucket, followed by the SD6060 modified and S2055 modified airfoils.

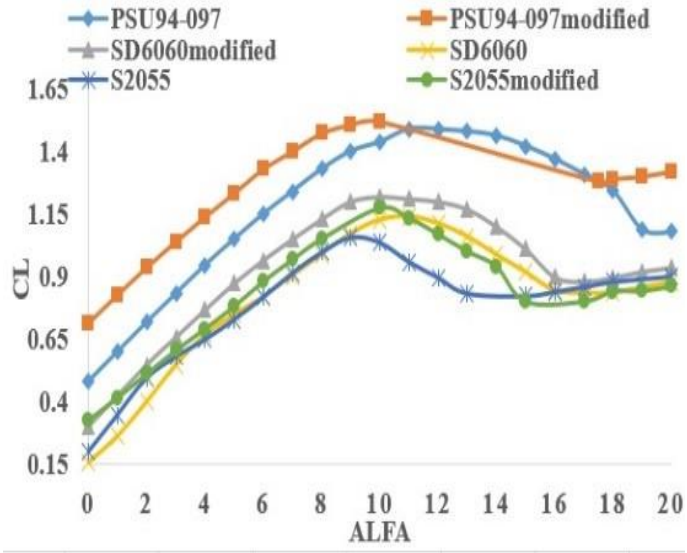

a) CL of base and modified airfoils

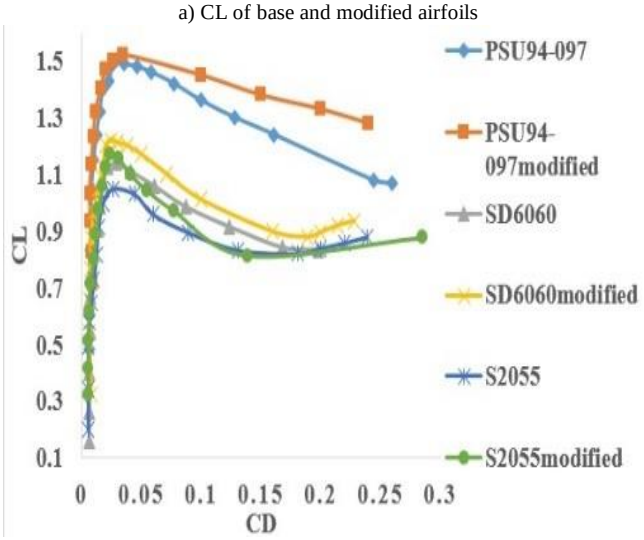

b) Drag buckets for base and modified airfoils

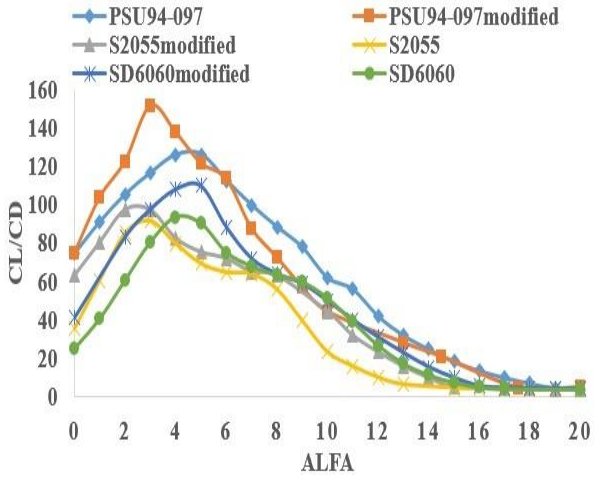

c) CL/CD performance of base and modified airfoils

Fig. 12. Comparison of CL, drag buckets, and CL/CD of base and modified airfoils at Re of 500,000

The CL/CD efficiency of the original and modified airfoils at a Re of 500,000 is illustrated in Fig. 12(c). In investigations for AoA from 0° to 4°, the PSU94-097 modified airfoil outperforms the base and other modified airfoils. While the peak CL/CD of the S2055 airfoil was 91.59 at an AoA of 3°, that of the PSU94-097 modified airfoil was 151.60. Similarly, the highest CL/CD values for the modified SD6060 and S2055 airfoils were

109.87 at an AoA of 5° and 97.13 at an AoA of 2°, respectively. For the PSU94-097 and SD6060 airfoils, the highest CL/CD values were 126.10 at an AoA of 5° and 93.32 at an AoA of 4°, respectively. Consequently, all modified airfoils exhibited a greater peak CL/CD than the basic airfoils.

3.3. Summary of performance and technical analysis

The lift and stall AoA data, as well as the CL/CD summary for the SD6060, SD6060 modified, S2055, S2055 modified, PSU94-097, and PSU94-097 modified airfoils, are shown in Figs 13 and 14, respectively. According to Figs. 13(a) and (b), among the modified airfoils, PSU94-097 had the highest peak CL at the studied Re range of 50,000 to 500,000, while S2055 had the lowest peak CL at the examined Re of 50,000. Additionally, the PSU94-097 modified airfoil also exhibited the highest peak CL across the Re range from 50,000 to 500,000. Conversely, the S2055 modified airfoil had the lowest peak CL among the modified airfoils at Re of 50,000, whereas the SD6060 modified airfoil had the lowest peak at Re from 75,000 to 500,000. As discussed previously, the base airfoils exhibited the lowest peak CL across all Re investigated, from 50,000 to 500,000. The stall AoA values for the modified airfoils ranged between 8° and 12°, with the maximum stall AoA observed at Re from 75,000 to 100,000 being 12°. Furthermore, at Re of 75,000, the stall AoA value of the PSU94-097 modified airfoil surpassed that of the PSU94-097 airfoil, while at other Re, the stall AoA values for both PSU94-097 and PSU94-097 modified airfoils were equal. For SD6060 and SD6060 modified airfoils, the stall AoA values at Re of 50,000, 75,000, 200,000, and 500,000 remained consistent. Additionally, the stall AoA value of the S2055 modified airfoil exceeded that of the base airfoil at Re of 100,000, 300,000, 400,000, and 500,000. Moreover, the stall AoA values of the S2055 modified and S2055 airfoils were equal at Re of 50,000 and 75,000.

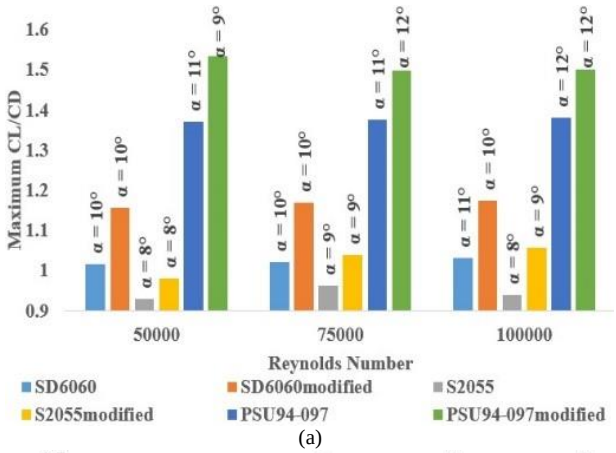

(a)

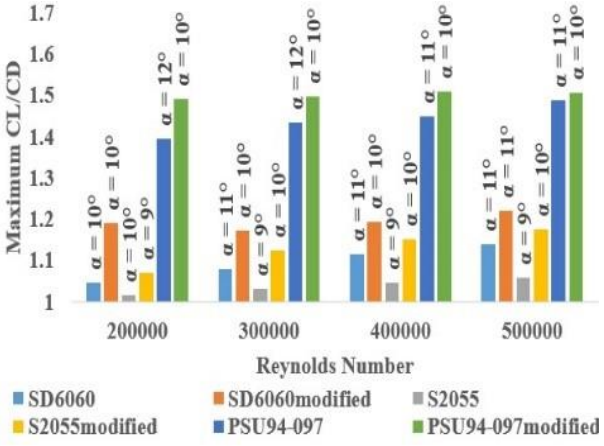

(b)

Fig. 13. Lift and stall AoA efficiency summary for all airfoils

Fig. 14 illustrates that as Re increases from 50,000 to 500,000, the peak CL/CD of all modified airfoils also increases. For each airfoil, the highest peak CL/CD is observed at Re of 500,000, while the lowest maximum CL/CD is observed at Re of 50,000. Across the investigated Re range of 50,000 to 500,000, the PSU94-097 modified airfoil exhibited a higher maximum CL/CD compared to other modified airfoils and base airfoils. The maximum CL/CD value for all modified and base airfoils was 151.60, observed for the PSU94-097 modified airfoil at Re of 500,000. Additionally, all modified airfoils demonstrated higher maximum CL/CD values compared to their respective base airfoils. Furthermore, among the modified airfoils, the SD6060 modified airfoil had the lowest maximum CL/CD value at Re of 75,000, while at Re of 50,000 and 100,000 to 500,000, the S2055 modified airfoil exhibited a lower maximum CL/CD compared to other modified airfoils.

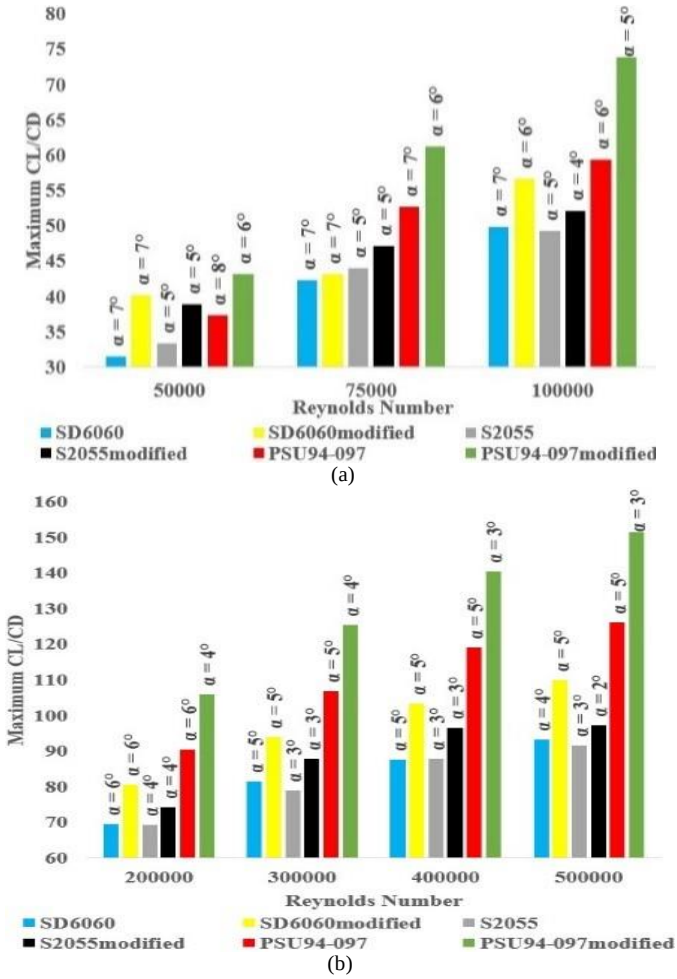

Fig. 14. CL/CD efficiency summary for entire airfoils

4. Conclusion

The present study investigated the aerodynamic efficiency characteristics of the PSU94-097, SD6060, and S2055 modified airfoils developed SWT usage using XFOIL at Re ≤ 500,000, a typical range for SWT airfoils. The results indicated that efficiency generally improved with increasing Re. The study yielded the following key findings:

1. Modifying the t/c range to 1.50 to 2.25 for the SD6060 airfoil enhances efficiency.
2. Efficiency increases when using the optimal t/c range of 2.25 to 3 with the S2055 airfoil.
3. Modifying the t/c limit to 0.60 to 1.50 for the PSU94-097 airfoil enhances efficiency.
4. The PSU94-097 modified airfoil achieved the highest peak CL/CD of 151.60 at Re of 500,000.
5. The peak CL/CD values for the SD6060 modified and S2055 modified airfoils were 109.87 and 97.1, respectively.
6. The peak CL values for the PSU94-097 modified, SD6060 modified, and S2055

modified airfoils were 1.534, 1.219, and 1.174, respectively.
7. The PSU94-097 modified airfoil also exhibited the highest peak CL at Re ranging from 50,000 to 500,000.
8. In drag bucket analyses, the entire modified airfoils increased CL efficiency to the point where CL peaked with either a constant or decreasing CD across all Re.
9. At Re ≤ 500,000, the PSU94-097 modified airfoil demonstrated a higher peak CL/CD compared to the other modified and base airfoils.
10. For the PSU94-097 modified airfoil, the peak CL/CD was found to be 15.8% at Re of 50,000, 16.08% at Re of 75,000, 24.43% at Re of 100,000, 17.12% at Re of 200,000, 17.30% at Re of 300,000, 17.98% at Re of 400,000, and 20.22% higher at Re of 500,000.
11. For the SD6060 modified airfoil, the peak CL/CD was presented as 27.87% at Re of 50,000, 2.03% at Re of 75,000, 13.77% at Re of 100,000, 15.83% at Re of 200,000, 15.14% at Re of 300,000, 17.95% at Re of 400,000, and 17.73% higher at Re of 500,000.
12. For the S2055 modified airfoil, the greatest CL/CD was recorded at 16.70% at Re of 50,000, 7.11% at Re of 75,000, 5.77% at Re of 100,000, 7.25% at Re of 200,000, 11.40% at Re of 300,000, 9.99% at Re of 400,000, and 6.04% higher at Re of 500,000.
Furthermore, the present study was validated with experimental results. The minimal variation in lift efficiency across all modified airfoils is suitable for analyzing SWT for low Re applications. Multiple experimental tests will accompany this study across the entire Re range. Subsequently, the developed and constructed 3-bladed horizontal axis wind turbine concept will undergo thorough CFD computations, particle image velocimetry (PIV) flow visualization, and wind tunnel testing.

Nomenclature	
Roman symbol	
c	Chord of length (m)
% c	Percentage of chord (-)
C_D	Drag Coefficient (-)
C_L	Lift Coefficient (-)
C_L/C_D	Lift-to-drag ratio (-)
C_P	Power coefficient (-)
D	Drag force (N)
l	Airfoil span (m)
L	Lift force (N)
Re	Reynolds number (-)
t/c	Thickness to camber ratio (-)
Acronyms	
AoA	Angle of Attack
BEMT	Blade Element Momentum Theory
CFD	Computational Fluid Dynamics
SWT	Small Wind Turbine
WT	Wind Turbine
Greek Symbol	
ρ	Airflow density (Kg/m^3)
μ	Dynamic viscosity (Kg $m^{-1}s^{-1}$)
υ	Kinematic viscosity (m^2s^{-1})

Acknowledgment

There has been no support from any organization to carry out this project.

References

Abdelwahed, K.S. & Abd El-Rahman, A.I., 2020. Shape optimization of SG6043 airfoil for small wind turbine blades. *Journal of Physics: Conference Series*, 1618(4), 042007. https://doi.org/10.1088/1742-6596/1618/4/042007.

Acarer, S., 2020. Peak lift-to-drag ratio enhancement of the DU12W262 airfoil by passive flow control and its impact on horizontal and vertical axis wind turbines. *Energy*, 201, 117659. https://doi.org/10.1016/j.energy.2020.117659

Akour, S.N., Al-Heymari, M., Ahmed, T. & Khalil, K.A., 2018. Experimental and theoretical investigation of micro wind turbine for low wind speed regions. *Renewable energy*, 116, 215-223. https://doi.org/10.1016/j.renene.2017.09.076

Badawy, Y.E., Nawar, M.A., Attai, Y.A. & Mohamed, M.H., 2023. Co-enhancements of several design parameters of an archimedes spiral turbine for hydrokinetic energy conversion. *Energy*, 268, 126715. https://doi.org/10.1016/j.energy.2023.126715

Bai, C.J., Wang, W.C., Chen, P.W. & Chong, W.T., 2014. System integration of the horizontal-axis wind turbine: The design of turbine blades with an axial-flux permanent magnet generator. *Energies*, 7(11), 7773-7793. https://doi.org/10.3390/en7117773

Bashir, M., Longtin Martel, S., Botez, R.M. & Wong, T., 2022. Aerodynamic shape optimization of camber morphing airfoil based on black widow optimization.

In AIAA Scitech 2022 Forum, 2575. https://doi.org/10.2514/6.2022-2575.vid

Bhavsar, H., Roy, S. & Niyas, H., 2023. Aerodynamic performance enhancement of the DU99W405 airfoil for horizontal axis wind turbines using slotted airfoil configuration. *Energy*, 263, 125666. https://doi.org/10.1016/j.energy.2022.125666

Leite, B., Afonso, F. & Suleman, A., 2022. Aerodynamic Shape Optimization of a Symmetric Airfoil from Subsonic to Hypersonic Flight Regimes. *Fluids*, 7(11), 353. https://doi.org/10.3390/fluids7110353

Lendraitis, M. & Lukoševičius, V., 2023. Novel Approach of Airfoil Shape Representation Using Modified Finite Element Method for Morphing Trailing Edge. *Mathematics*, 11(9), 1986. https://doi.org/10.3390/math11091986

Longtin Martel, S., Bashir, M., Botez, R.M. & Wong, T., 2023. A Pareto Multi-Objective Optimization of a Camber Morphing Airfoil using Non-Dominated Sorting Genetic Algorithm. *In AIAA SCITECH 2023 Forum*, 1583. https://doi.org/10.2514/6.2023-1583

Karthikeyan, N., Murugavel, K.K., Kumar, S.A. & Rajakumar, S., 2015. Review of aerodynamic developments on small horizontal axis wind turbine blade. *Renewable and Sustainable Energy Reviews*, 42, 801-822. https://doi.org/10.1016/j.rser.2014.10.086

Kumar, S. & Narayanan, S., 2022. Airfoil thickness effects on flow and acoustic characteristics. *Alexandria Engineering Journal*, 61(6), 4679-4699. https://doi.org/10.1016/j.aej.2021.10.022

Maughmer, M.D., Swan, T.S. & Willits, S.M., 2002. Design and testing of a winglet airfoil for low-speed aircraft. *Journal of Aircraft*, 39(4), 654-661. https://doi.org/10.2514/2.2978

Nemati, M. & Jahangirian, A., 2020. Robust aerodynamic morphing shape optimization for high-lift missions. *Aerospace Science and Technology*, 103, 105897. https://doi.org/10.1016/j.ast.2020.105897

Porto, H.A., Fortulan, C.A. & Porto, A.V., 2022. Power performance of starting-improved and multi-bladed horizontal-axis small wind turbines. *Sustainable Energy Technologies and Assessments*, 53, 102341.

Renganathan, S.A., Maulik, R. & Ahuja, J., 2021. Enhanced data efficiency using deep neural networks and Gaussian processes for aerodynamic design optimization. *Aerospace Science and Technology*, 111, 106522. https://doi.org/10.1016/j.ast.2021.106522

Salinas, M.F., Botez, R.M. & Gauthier, G., 2023. New validation methodology of an adaptive wing for UAV S45 for fuel reduction and climate improvement. *Applied Sciences*, 13(3), 1799. https://doi.org/10.3390/app13031799

Sarkar, D., Shukla, S., Alom, N., Sharma, P. & Bora, B.J., 2023. Investigation of a newly developed slotted bladed darrieus vertical Axis wind turbine: A numerical and response surface methodology analysis. *Journal of Energy Resources Technology*, 145(5), 051302. https://doi.org/10.1115/1.4056331

Seifi, H., Kouravand, S., Davary, M.S. & Mohammadzadeh, S., 2023. Numerical and Experimental study of the effect of increasing aspect ratio of self-starting force to vertical axis wind turbine. *Journal of Renewable and New Energy*, 10(1), 1-14. https://doi.org/10.52547/JRENEW.10.1.1

Seifi, H., Kouravand, S. & Seifi Davary, M., 2023. Numerical and experimental study of NACA airfoil in low Reynolds numbers for use of Darriues vertical axis micro-wind turbine. *Journal of Renewable and New Energy*, 10(2), 149-163. https://doi.org/10.52547/JRENEW.10.2.149

Seifi Davari, H., Chowdhury, H., Seify Davari, M. & Hosseinzadeh, H., 2024. Optimizing airfoil efficiency for offshore turbines through aerodynamic geometry enhancement. *Mathematical Analysis and its Contemporary Applications*. https://doi.org/10.30495/maca.2024.2017221.1092

Seifi Davari, H., Seify Davari, M., Kouravand, S. & Kafili Kurdkandi, M., 2024. Optimizing the Aerodynamic Efficiency of Different Airfoils by Altering Their Geometry at Low Reynolds Numbers. *Arabian Journal for Science and Engineering*, 1-36. https://doi.org/10.1007/s13369-024-08944-4

Seifi Davari, H., Kouravand, S., Seify Davari, M. & Kamalnejad, Z., 2023. Numerical investigation and aerodynamic simulation of Darrieus H-rotor wind turbine at low Reynolds numbers. *Energy Sources, Part A: Recovery, Utilization, and Environmental Effects*, 45(3), 6813-6833. https://doi.org/10.1080/15567036.2023.2213670

Seifi Davari, H., Seify Davari, M., Botez, R. & Chowdhury, H., 2023. Maximizing the Peak Lift-To-Drag Coefficient Ratio of Airfoils by Optimizing the Ratio of Thickness to the Camber of Airfoils. *Sustainable Earth Trends*, 3(4), 46-61. https://doi.org/10.48308/SER.2024.234811.1036

Song, Q. & David Lubitz, W., 2014. Design and testing of a new small wind turbine blade. *Journal of solar energy engineering*, 136(3), 034502. https://doi.org/10.1115/1.4026464

Tang, X., Yuan, K., Gu, N., Li, P. & Peng, R., 2022. An interval quantification-based optimization approach for wind turbine airfoil under uncertainties. *Energy*, 244, 122. https://doi.org/10.1016/j.energy.2021.122623

Tanürün, H.E., 2024. Improvement of vertical axis wind turbine performance by using the optimized adaptive flap by the Taguchi method. *Energy Sources, Part A: Recovery, Utilization, and Environmental Effects*, 46(1), 71-90. https://doi.org/10.1080/15567036.2023.2279264

Tarhan, C. & Yilmaz, I., 2019. Numerical and experimental investigations of 14 different small wind turbine airfoils for 3 different reynolds number conditions. *Wind and Structures*, 28(3), 141-153. https://doi.org/10.12989/was.2019.28.3.141

Wei, X., Wang, X. & Chen, S., 2020. Research on parameterization and optimization procedure of low-Reynolds-number airfoils based on genetic algorithm and Bezier curve. *Advances in Engineering Software*, 149, 102864. https://doi.org/10.1016/j.advengsoft.2020.102864

Zargar, O.A., Lin, T., Zebua, A.G., Lai, T.J., Shih, Y.C., Hu, S.C. & Leggett, G., 2022. The effects of surface modification on aerodynamic characteristics of airfoil DU 06 W 200 at low Reynolds numbers. *International Journal of Thermofluids*, 16, 100208. https://doi.org/10.1016/j.ijft.2022.100208.